A Flow-Field Guided Method of Path Planning for Unmanned Ground Vehicles

Nan Wang[1], Mengxuan Song[1], Jun Wang[1*], and Timothy Gordon[2]

***Abstract*— This paper focuses on the path planning problem for unmanned ground vehicles in complex environments. Fluid flow is applied to the path planning method based on the natural ability of the fluid in finding its outlet. The proposed method consists of two layers: the flow-field layer and the optimization layer. The flow-field layer provides a velocity distribution which describes the fluid flowing from a starting point to a terminal point. The solution of the flow field is obtained by the method of computational fluid dynamics. The optimization layer generates a specific path and guarantees the feasibility of the path. The proposed method is verified in several scenarios, and the smoothness and the completeness of the generated path is well demonstrated.**

I. Introduction

sampling-based In recent years, the path planning problem for Unmanned Ground Vehicles (UGVs) has attracted much attention. The reference path influences the performance of the control module significantly. One of the key challenges in path planning is generating a smooth path in complex environments subject to non-holonomic constraints.

Various path planning methods have been developed. Conventional graph search algorithms, such as the Dijkstra algorithm [1], the A* algorithm [2] and the D* algorithm [3], search the global map for a path. But graph search algorithms are designed only for holonomic systems, and are not suitable for UGV applications.

Artificial intelligence algorithms including the fuzzy logic [4], the genetic [5] and the neural-networks [6] algorithms have been successfully implemented in path planning. These methods can handle the constraints of vehicle kinematics and environment, but cannot always guarantee feasible solutions. Similar methods such as model-based optimization algorithm [7] are also proposed, which share the same drawbacks.

Further efforts have been devoted to sampling-based planners such as the rapidly-exploring randomized tree [8] and the probabilistic road map [9]. One key drawback of the sampling-based method is that the probabilistic completeness is achieved only when the number of samples approaches infinity. Besides, they are not appropriate for non-holonomic systems.

The method of Artificial Potential Field (APF) [10] is another conventional method for path planning. It provides a smooth and collision-free path. But the local minima in the potential field make it inappropriate for path planning in complex environments [11]. The traditional APF method consists of two steps, i.e. define a function of potential field and simulate a particle moving according to the potential field. The APF methods have been improved to deal with their drawback. Most improvement focused on the process of path following [12]. The following research modified the definition of the potential field. Reference [13] proposed a rotational potential field to avoid being stuck in local minima by making the repulsive force tangent to the potential field. Only the case with a single convex obstacle is considered and the feasibility in complex scenarios remains unconfirmed. Reference [14] proposed a harmonic potential field to guide the particle. In the field, no local minima exist even when there are multiple convex obstacles. But all the obstacles have to be expanded to spheroids, which wastes free space. Therefore the problems are rendered unsolvable in narrow space.

All the methods mentioned above cannot achieve good performance of smoothness and completeness simultaneously. Reference [15] proposed a path planning method which makes use of the vector field analysis. Reference [16] for the first time appllied the fluid flow to the path planning field. The results showed good performance in terms of smoothness and completeness.

In this paper, a geometric method is proposed to directly express the differences between the fluid flow and the vehicle movement. Besides, a stronger constraint is added to avoid the collision than the previous work. Fluid flow has many properties that can be used to provide the guidance. (1) According to the law of conservation of mass, fluid will always flow out of outlets if incompressible fluid flows into an inlet. (2) It is demonstrated that fluid always moves along a collision-free path. (3) The flow field is smooth.

The paper is structured as follows: Section II describes the hypothesis, governing equations and boundary conditions in the flow-field layer. Section III presents details about the optimization layer including the vehicle model, the cost function and the optimization process. Section IV gives results to demonstrate the performance of the proposed method. Finally, Section V summarizes the contributions of the paper and maps out future research directions.

II. Flow-Field Layer

The overall structure of the proposed method consists of two layers. The top layer generates a flow field within free space by Computational Fluid Dynamics (CFD) using

This work was supported in part by the National Natural Science Foundation of China (NSFC) under Grant No. 61473209 and No. 61773291.

[1]Nan Wang, Mengxuan Song and Jun Wang are with the Department of Control Science and Engineering, Tongji University, Shanghai 201804, P.R.China.

[2]Timothy Gordon is with the School of Engineering, University of Lincoln, Lincoln, Lincolnshire, UK.

*Corresponding author: junwang@tongji.edu.cn.

the software of ANSYS. The bottom layer develops an optimization method to find a feasible path. In this paper, vehicle model is used in three aspects: (1) analysis of velocity distribution on vehicle body; (2) update of vehicle states; (3) model constraints in optimization process. As an essential component in the optimization layer, the cost function consists of two terms. One term guides a simulated vehicle to follow the fluid flow, and the other avoids collisions. The optimization problem is solved in a receding manner. The steering angle is obtained at each step. A specific path is calculated based on the sequence of steering angles.

One of the most novel parts of this paper is using a fluid flow as guidance. In this section, a brief description about CFD is presented.

A. Hypothesis

The CFD is introduced not to simulate a realistic fluid phenomenon, but to provide a reference for path planning. Therefore the fluid matter is merely imaginary, and several hypothesis and simplifications should be made during the generation of the flow field. (1) Due to the requirement of smoothness of the path, flow field with turbulence would not make a good candidate. Therefore the flow field is purely laminar, and its Reynolds number would be sufficiently low. (2) In order to obtain consistent path planning strategy for all possible circumstances, boundary conditions for solving the flow field should not be intervened by any case-specific adjustments, but determined by the starting point, the target point and the obstacles only. (3) The discretized mesh of the computational domain does not need to be refined to resolve boundary layers, and in the mean time, it must be fine enough to provide smooth interpolations for the vehicle movement.

Although other properties of the fluid remain uncertain, some simplified settings are used, for that our concern is whether the flow field can provide a good reference for path planning rather than resolve real physical phenomenon. (1) Physical properties of the fluid are constant. (2) The fluid is incompressible. (3) The gravitational force is not considered.

B. Governing equations

With the hypothesis and simplification described above, the governing equations of the fluid flow are the continuum equation and the momentum conservation equation, as listed below.

$$\nabla \mathbf{u} = 0, \tag{1}$$

$$\rho \mathbf{u} \cdot \nabla \mathbf{u} = -\nabla p + \nabla \cdot (\mu \nabla \mathbf{u}), \tag{2}$$

where $\mathbf{u}$ is the velocity vector, ρ is the fluid density, μ is the molecular viscosity. In the present study, the values are chosen according to the air under normal state.

C. Boundary conditions

The boundary conditions for solving the flow field are set as follows. (1) The wall behind the vehicle at the starting point has uniform velocities at a fixed value (10^{-5} m/s in the present study), with directions perpendicular to the wall and pointing into the domain. (2) The wall in front of the vehicle at the terminal point is set as a fully developed outlet. (3) Other walls are no-slip solid borders.

D. CFD Simulation

1) Mesh generation: A mesh has to be generated to discretize the calculation domain. ANSYS ICEM CFD is employed to achieve the aim. The density of the nodes has to guarantee that the vehicle body covers moderate number of nodes. If the vehicle body covers too few nodes, the generated path will be unsmooth. If the vehicle body covers too many nodes, the burden of computation will be unnecessarily increased.

In Figure 1, an 80-m×60-m map is taken as an example where 55926 nodes are generated. Considering a normal vehicle with length of 4.5 m and width of 1.8 m, the vehicle body occupies about 94.38 nodes on average.

2) Fluid flow calculation: ANSYS Fluent is employed to calculate the velocity distribution in the flow field.

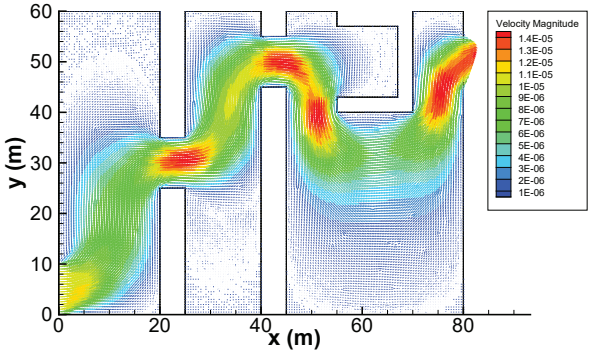

Fig. 1. Flow field in Scenario 1

III. Optimization Layer

The purpose of the optimization layer is to obtain a feasible path in the fluid flow. Three key factors must be taken into account: (1) non-holonomic velocity constraints, (2) rigidity of the vehicle and (3) collision avoidance. The first factor is formulated as a specific constraint by employing the vehicle model. The remaining two factors are modelled into a cost function. The path is obtained by solving the optimization problem in a receding manner, .

A. Vehicle model

The vehicle model is shown in Figure 2. Maneuvers are assumed to have zero sideslip angles. The state of the model is $\mathbf{X}(t) = [x(t), y(t), \theta(t)]$, where $x(t)$ and $y(t)$ are the coordinates of the middle point of the rear axle in a global coordinate system and $\theta(t)$ is the heading angle of the vehicle body with respect to the x axis. The input of the system is $[v, \delta(t)]$, of which v is the longitudinal velocity and $\delta(t)$ is the steering angle of the front wheels. l is the distance between the front axle and rear axle. The vehicle model is:

$$\begin{cases} \dot{x} = v\cos\theta \\ \dot{y} = v\sin\theta \\ \dot{\theta} = v\frac{\tan\delta}{l} \end{cases}, \tag{3}$$

where $|\delta(t)| \leq \delta_{\max}$.

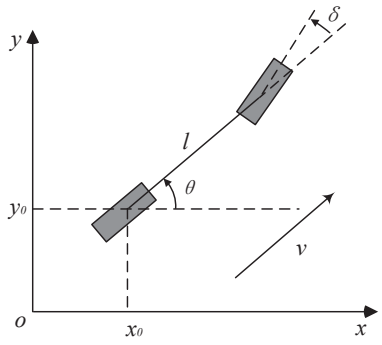

Fig. 2. The vehicle model

If the wheel turns to the left side, $\delta(t) > 0$. Assuming that the longitudinal velocity is constant, the state $\mathbf{X}(t+\Delta t)$ can be calculated based on current state $\mathbf{X}(t)$ and input $\delta(t)$:

$$\begin{cases} x(t+\Delta t) = x(t) + v\Delta t \cos\theta(t) \\ y(t+\Delta t) = y(t) + v\Delta t \sin\theta(t) \\ \theta(t+\Delta t) = \theta(t) + v\Delta t \frac{\tan\delta(t)}{l} \end{cases}. \tag{4}$$

B. Cost function

A feasible reference path is generated by minimizing the value of the cost function in the receding manner. The cost function includes the term of the differences from the flow field and the term of collision emergency.

1) Difference from the fluid flow: The differences between the velocity distribution of the vehicle body and that of the fluid flow should be minimized. The velocity distribution of the vehicle body is calculated based on the input $\delta(t)$, geometric deduction and the vehicle model.

In the deduction, let i denotes any node covered by the vehicle body. $\mathbf{v}_i$ is the velocity of vehicle body at node i. $\mathbf{v}_i{}'$ is the velocity of the fluid flow at node i. $< \mathbf{v}_i, \mathbf{v}_i' >$ describes the included angle at node i. Ω_t represents the point set within the vehicle body at state $\mathbf{X}(t)$. As is shown in Figure 3, the mean value of the differences of all the nodes within Ω_t represents the differences between the vehicle and the flow. N_t represents the number of the nodes. The cost function in terms of coherence is defined as

$$F_d = \frac{1}{N_t} \sum_{i \in \Omega_t} < \mathbf{v}_i, \mathbf{v}_i' > . \tag{5}$$

The blue arrows in Figure 3 represent the velocity distribution of the fluid flow and the red arrows represent that of the vehicle body.

2) Collision emergency: The collision occurs when the vehicle body overlaps the obstacle. A penalty value is used to punish the overlap. The penalty value is set to be a relatively large value P.

$$F_c = \begin{cases} 0 & \text{if collision is not detected} \\ \mathrm{P} & \text{if collision is detected} \end{cases}. \tag{6}$$

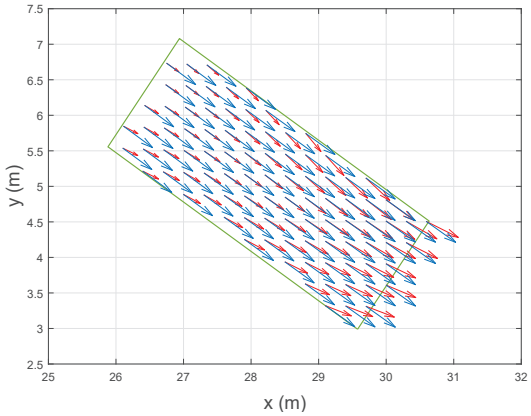

Fig. 3. Differences between velocity distribution of the vehicle body and that of the flow field

TABLE I
PARAMETERS TABLE

Parameters	Values	Units
Length	4.50	m
Width	1.86	m
Wheelbase	2.65	m
δmax	28.2	deg

C. Optimization Problem

To obtain a feasible reference path without collisions, the following problem is solved at each step.

The objective function is

$$\min_{\delta} F = F_d + F_c. \tag{7}$$

The constraint of input is

$$|\delta| \leq \delta_{\max}. \tag{8}$$

The interior-point method is used to solve the minimization problems. The optimization problems are solved by the function *fmincon* in Matlab Optimization Toolbox. According to the solution δ and velocity v, the state of vehicle is updated by Equation (4). The iteration will not stop until the distance between the current position and the terminal position is less than a threshold.

IV. SIMULATION AND RESULTS

The performance of the proposed path planning method is verified in typical scenarios. Details about the simulation and results are described in this section.

A. Simulation Setup

As Table I shows, the parameters of the vehicle model are derived from an experiment vehicle in our lab.

Six scenarios are designed in the simulation:

- A complex maze;
- Merging while avoiding obstacles;
- U-turn;
- Turning left at an intersection;
- Leaving a parking slot;

- Leaving a warehouse.

The first scenario demonstrates that the proposed method is able to generate a path in a complex map with concave obstacles. The second scenario confirms that the path is relatively smooth. The rest four scenarios are designed to simulate some practical situations.

B. Simulation Results

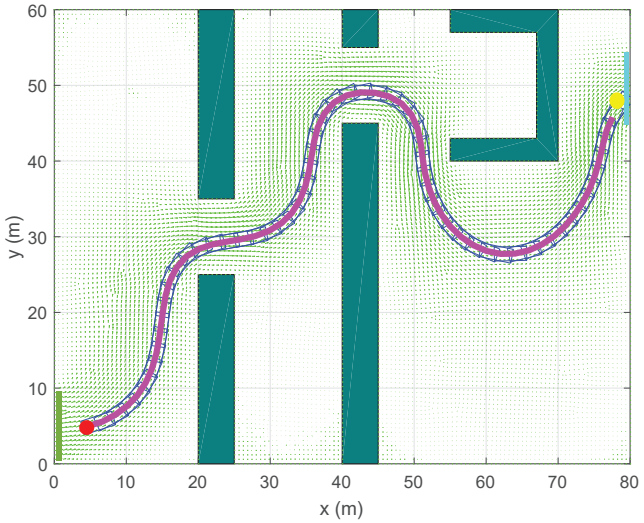

Fig. 4. The generated path in Scenario 1

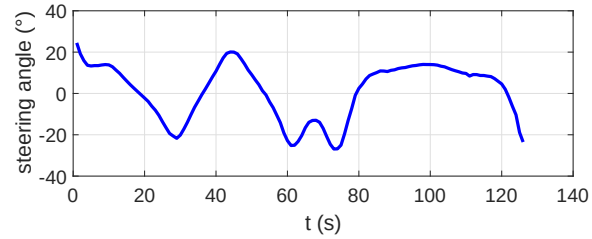

(a) Front wheel steering angle

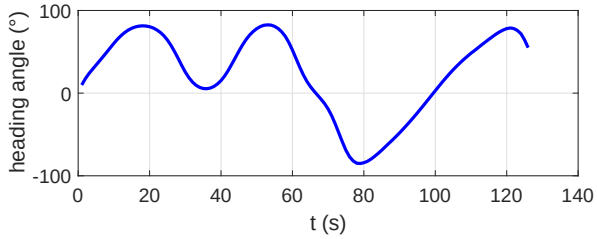

(b) Heading angle

Fig. 5. Indices in Scenario 1

The flow field in Scenario 1 is shown in Figure 1. Figure 4 presents the generated path of the proposed method. The dark green rectangles in Figure 4 represent obstacles. The red dot represents starting point and the yellow dot represents the terminal point. The green rectangle represents the inlet and the light blue rectangle represents the outlet. The light green arrows represent the velocity distribution of the flow field.

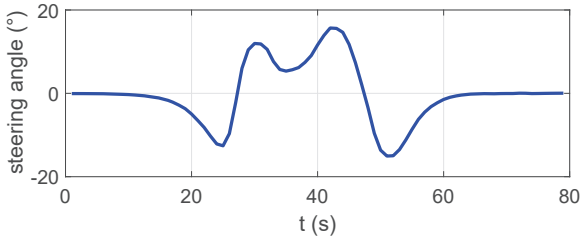

(a) Front wheel steering angle

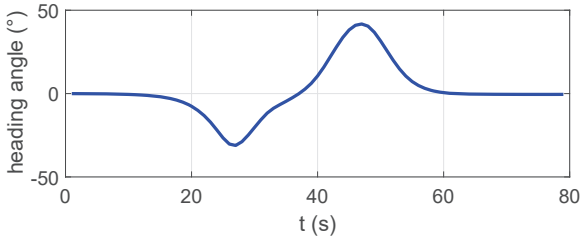

(b) Heading angle

Fig. 8. Indices in Scenario 2

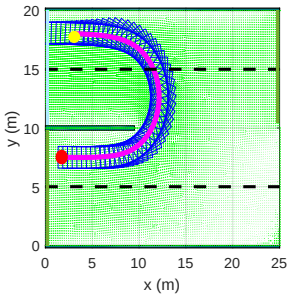

(a) Scenario 3: u-turn

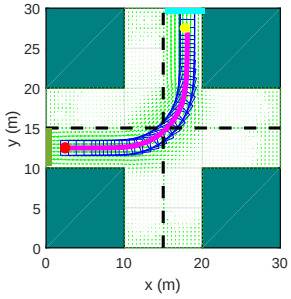

(b) Scenario 4: turning left at an intersection

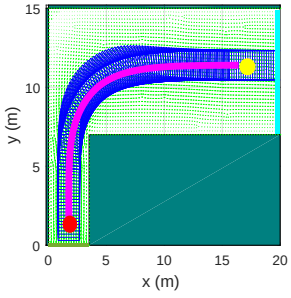

(c) Scenario 5: leaving a parking lot

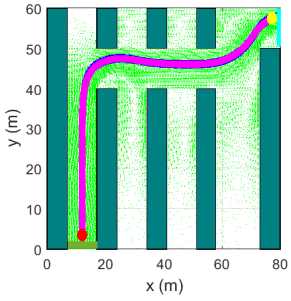

(d) Scenario 6: leaving a warehouse

Fig. 9. The generated path in the remaining four scenarios

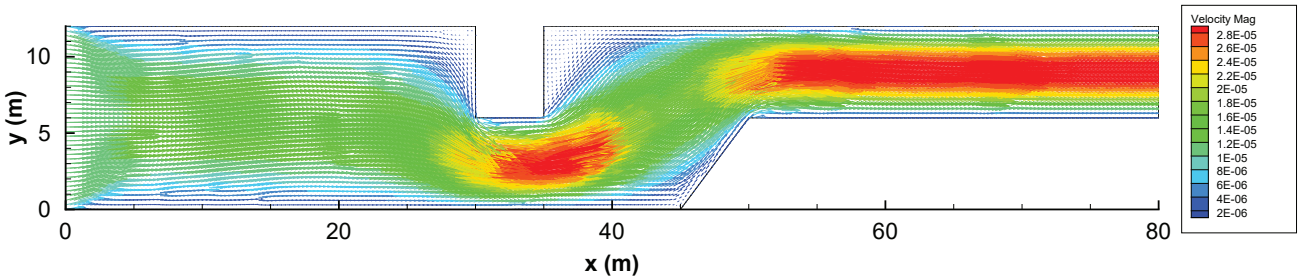

Fig. 6. Flow field in Scenario 2

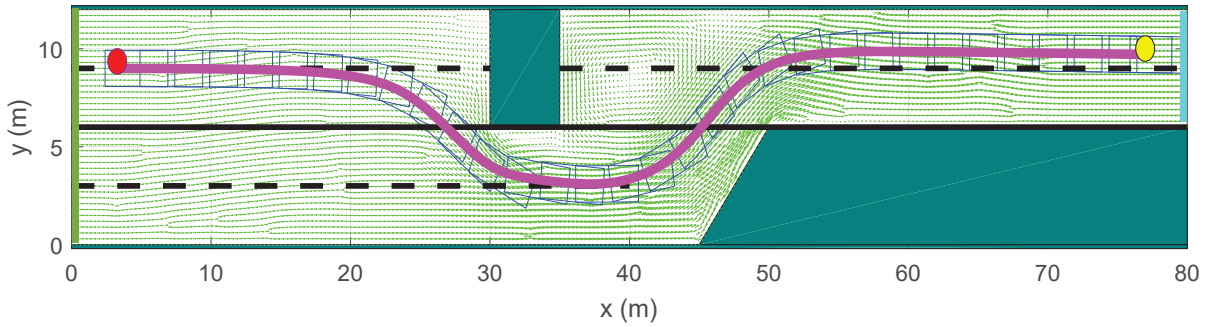

Fig. 7. The generated path in Scenario 2

TABLE II
PERFORMANCE IN EACH SCENARIOS

Scenario No	Longitude velocity (m/s)	Length (m)	Mean value of absolute angular velocity (deg/s)	Standard deviation of absolute angular velocity (deg/s)	Maximum of absolute angular velocity (deg/s)
1	1	125	4.64	2.53	11.0
2	1	78	1.86	2.00	6.07
3	1	25	7.22	4.73	11.6
4	1	26	3.45	3.06	7.22
5	0.2	22	0.818	0.855	2.32
6	1	107	1.68	1.96	7.68

The dark blue lines represent the vehicle body at each frame. The purple curve represents the generated path. The path is implied to be collision-free in this case because no overlap exists between the obstacles and the vehicle. The path does not get trapped in concave obstacles while other methods may fail.

The steering angles of the front wheels and the heading angles during the simulation are shown in Figures 5(a) and 5(b). The steering angles during the simulation are within the range of $[-\delta_{\max}, \delta_{\max}]$. The curve of the heading angles in the experiment is smooth.

Scenario 2 is presented to simulate the situation when car merges into an adjacent lane while avoiding the obstacles. Figures 6, 7 and 8 show the flow field, the generated path and the indices in Scenario 2 respectively.

The length of the path is used to evaluate the efficiency. Assuming that the longitudinal velocity of the vehicle is constant, the heading angle can not change sharply for the smoothness requirement. The mean value and standard deviation of absolute angular velocity represent the variation of the heading angle. The maximum of the absolute angular velocity represents the sharpest change of the heading angle. All of the three indices are essential in quantifying the smoothness of the path.

The remaining results are shown in Figure 9. The proposed method is demonstrated to be applicable to various scenarios. Particularly, the result in Figure 9(c) implies that the method also works in limited space. The longitudinal velocity in Figure 9(c) is set relatively low for its higher requirement on precision. Table II shows the performance in all the scenarios. As is shown in Table II, the mean value, the standard deviation and the maximum of angular velocity in all the scenarios are at low level, which illustrates its smoothness.

V. CONCLUSIONS

In this paper, a path planning method is designed for UGVs by utilizing the properties of the fluid flow. The main advantages of the method are the abilities to solve complex geometric problems and to generate smooth and collision-free path for non-holonomic systems.

There are still outstanding problems to be solved. The solution of the optimization problem may lead to collisions If the fluid flow is divided into two branches. In addition, the inlet and outlet in the current formulation are set manually and should be set automatically in the future.

REFERENCES

[1] E. W. Dijkstra, "A note on two problems in connexion with graphs," *Numerische Mathematik*, vol. 1, no. 1, pp. 269–271, 1959.

[2] A. Stentz, "Optimal and efficient path planning for partially-known environments," in *IEEE International Conference on Robotics and Automation*, 1994, pp. 3310–3317.

[3] M. Likhachev, D. I. Ferguson, G. J. Gordon, A. Stentz, and S. Thrun, "Anytime dynamic A*: An anytime, replanning algorithm," in *The International Conference on Automated Planning and Scheduling*, 2005, pp. 262–271.

[4] A. Saffiotti, "The uses of fuzzy logic in autonomous robot navigation," *Soft Computing*, vol. 1, no. 4, pp. 180–197, 1997.

[5] K. H. Sedighi, K. Ashenayi, T. W. Manikas, R. L. Wainwright, and H.-M. Tai, "Autonomous local path planning for a mobile robot using a genetic algorithm," in *Evolutionary Computation*, vol. 2, 2004, pp. 1338–1345.

[6] M. J. Phinni, A. Sudheer, M. RamaKrishna, and K. Jemshid, "Obstacle avoidance of a wheeled mobile robot: A genetic-neurofuzzy approach," in *IISc Centenary-International Conference on Advances in Mechanical Engineering*, 2008.

[7] C. Li, J. Wang, X. Wang, and Y. Zhang, "A model based path planning algorithm for self-driving cars in dynamic environment," in *Chinese Automation Congress*, 2015, pp. 1123–1128.

[8] S. M. LaValle and J. James J. Kuffner, "Randomized kinodynamic planning," *The International Journal of Robotics Research*, vol. 20, no. 5, pp. 378–400, 2001.

[9] L. E. Kavraki, P. Svestka, J. C. Latombe, and M. H. Overmars, "Probabilistic roadmaps for path planning in high-dimensional configuration spaces," *IEEE Transactions on Robotics and Automation*, vol. 12, no. 4, pp. 566–580, 1996.

[10] O. Khatib, "Real-time obstacle avoidance for manipulators and mobile robots," in *Autonomous robot vehicles*, 1986, pp. 396–404.

[11] G. Li, S. Tong, G. Lv, R. Xiao, F. Cong, Z. Tong, A. Yamashita, and H. Asama, "An improved artificial potential field-based simultaneous forward search (Improved APF-based SIFORS) method for robot path planning," in *the 12th International Conference on Ubiquitous Robots and Ambient Intelligence*, 2015, pp. 330–335.

[12] M.-H. Kim, J.-H. Heo, Y. Wei, and M.-C. Lee, "A path planning algorithm using artificial potential field based on probability map," in *the 8th International Conference on Ubiquitous Robots and Ambient Intelligence*, 2011, pp. 41–43.

[13] H. Rezaee and F. Abdollahi, "Adaptive artificial potential field approach for obstacle avoidance of unmanned aircrafts," in *IEEE/ASME International Conference on Advanced Intelligent Mechatronics*, 2012, pp. 1–6.

[14] D. Lau, J. Eden, and D. Oetomo, "Fluid motion planner for nonholonomic 3-D mobile robots with kinematic constraints," *IEEE Transactions on Robotics*, vol. 31, no. 6, pp. 1537–1547, 2015.

[15] T. J. Gordon, M. C. Best, and P. J. Dixon, "An automated driver based on convergent vector fields," *Proceedings of the Institution of Mechanical Engineers, Part D: Journal of Automobile Engineering*, vol. 216, no. 4, pp. 329–347, 2002.

[16] M. Song, N. Wang, J. Wang, and T. Gordon, "A fluid dynamics approach to motion control for rigid autonomous ground vehicles," *the 25th International Symposium on Dynamics Vehicles on Roads and Tracks*, 2017.